

**Design of a bidirectional converter for charging/discharging a supercapacitor****Diseño de un convertidor bidireccional para la carga/descarga de un supercapacitor**

GARZA-GONZÁLEZ, Williams†\*, DURÁN-GÓMEZ, José Luis, LÓPEZ-FLORES, David Ricardo and SÁENZ-VALVERDE, David Alberto

*Tecnológico Nacional de México campus Chihuahua, México.*

ID 1<sup>st</sup> Author: Williams, Garza-González / **ORC ID:** 0000-0001-9668-7780, **CVU CONACYT ID:** 1079314

ID 1<sup>st</sup> Co-author: José Luis, Durán-Gómez / **ORC ID:** 0000-0003-0904-7828, **CVU CONAHCYT ID:** 11985

ID 2<sup>nd</sup> Co-author: David Ricardo, López-Flores / **ORC ID:** 0000-0003-4016-0845, **CVU CONAHCYT ID:** 250204

ID 3<sup>rd</sup> Co-author: David Alberto, Sáenz-Valverde / **ORC ID:** 0009-0007-7729-4077, **CVU CONAHCYT ID:** 1202447

**DOI:** 10.35429/JEE.2023.18.7.31.39

Received January 25, 2023; Accepted June 30, 2023

**Abstract**

This article presents the analysis and design of a new converter that combines the current doubler topology and the parallel converter to achieve greater stability and effective reduction of ripple in both voltage and current parameters. Basically, the DC-DC (Direct Current to Direct Current) converter operates with pulse modulators to control the current in the desired charging or discharging direction. Extensive simulations were carried out at nominal values of 48 V and 8.5 A of output, and 100 V of input to confirm the performance of this converter. The approach used has benefits in terms of safety, reduced electrical noise, practical implementation for interconnecting energy sources with high voltage ratios, and increased lifespan of supercapacitors as well as batteries. Simulation results are presented and the advantages and applications of this new configuration are discussed.

**Resumen**

Este artículo presenta el análisis y diseño de un nuevo convertidor que combina la topología del doblador de corriente y el convertidor paralelo para lograr una mayor estabilidad y una reducción efectiva del rizo en ambos parámetros de tensión y corriente. Básicamente el convertidor de CD-CD (Corriente directa a corriente directa) operara con moduladores de pulso para dirigir la corriente en el sentido deseado de carga o descarga. Se realizaron extensas simulaciones en valores nominales de 48 V y 8.5 A de salida, y 100 V de entrada para confirmar el rendimiento de este convertidor. El enfoque utilizado tiene beneficios en términos de seguridad, menor ruido eléctrico, una implementación práctica para interconectar fuentes de energía con altas relaciones de tensión y un aumento en la vida útil de los supercapacitores, así como de baterías. Se presentan los resultados de simulación y se discuten las ventajas y aplicaciones de esta nueva configuración.

**Supercapacitor, Bidirectional, Energy****Supercapacitor, Bidireccional, Energía**

**Citation:** GARZA-GONZÁLEZ, Williams, DURÁN-GÓMEZ, José Luis, LÓPEZ-FLORES, David Ricardo and SÁENZ-VALVERDE, David Alberto. Design of a bidirectional converter for charging/discharging a supercapacitor. Journal Electrical Engineering. 2023. 7-18:31-39.

\* Correspondence to Author (E-mail: M20061554@chihuahua.tecnm.mx)

† Researcher contributing as first author.

## Introduction

Today, new technological developments and population growth have led to a significant increase in global electricity consumption. As a result, fossil fuel-based sources of electricity such as gas, oil and coal have increased to meet the world's electricity consumption. Consequently, the environment has been adversely affected due to the increase in greenhouse gases. One alternative to reduce this effect is renewable energy sources (RESs) such as solar or wind power. However, due to the fluctuating and intermittent nature of RESs, it is necessary to equip them with energy storage systems (ESS) to improve their overall efficiency, reliability, and power quality (Hidalgo-Reyes et al., 2019).

For this reason, energy storage devices are becoming very essential elements to take advantage of these renewable energy sources; because their purpose is to store energy for use in times when energy is not produced and thus increase the efficiency of the system. Among all these devices are supercapacitors, which are a technology that is capable of delivering high power pulses in an instant of time; in addition to supporting a large number of charge and discharge cycles as well as providing high efficiency during this process, but despite this they have the disadvantage of being unable to maintain the same voltage for a long time. (Hidalgo-Reyes et al., 2019), due to the above described, power converters are required to regulate to a certain desired voltage.

Direct current to direct current (dc-dc) converters are now being widely used in such applications, since they can be used both to store energy and to help the system deliver energy when it is not generating it, thus offering greater autonomy to power grids, as well as superior sustainability to renewable energy sources.

In recent years, different configurations of bidirectional DC-DC converters have been proposed for supercapacitors. In (Rico-Secades et al., 2016) elaborated a one-branch bidirectional converter (switch array) for charging and discharging two battery modules, using complementary pulse modulator (PWM) circuits in the transistors used; thus allowing that with a small duty cycle the battery is discharged and a larger duty cycle will cause its respective charge.

At (Huang et al., 2018; Ibanez et al., 2013; Kim & Sul, 2006) they propose a 3-branch and 4-branch step-up parallel converter, each branch uses the same duty cycle, but has an offset of 120 and 90 degrees respectively between each of them, this with the purpose of reducing the ripple of the current in the supercapacitors and even if one of the branches presents a failure, the system will be able to remain operational. In (López-Flores et al., 2010) present a phase-shifting full-bridge converter, in which they use the current doubler to be able to deliver a greater amount of current while helping to reduce the ripple, although it depends on the duty cycle used. There are also (Kayaalp et al., 2016; Lai et al., 2016; Shreelekha & Arulmozhi, 2016; Zhixiang Ling et al., 2015) which use phase-shift control, rather than duty-cycle control, thus enabling their more efficient use in multiport systems; (Rahimpour & Baghrmian, 2017; Zakis et al., 2012) use the Z-source and  $\Gamma$ -source topologies for greater voltage and current stability, while reducing the reactive components of the circuit.

The previously analyzed works present appropriate activation methods for the switches of bidirectional dc-dc converters, and thus properly achieve the stability of the operating voltage and current at terminals with an acceptable ripple in both parameters. However, the ripple in the operating voltage and current can be variable and higher.

This paper presents a converter in which the current doubler topology is used in conjunction with the parallel converter topology (Figure 1), where the latter will operate at a duty cycle close to 0.5. Moreover, complementary PWMs circuits are used for a simple and efficient control of the charging and discharging of a supercapacitor (Not addressed in this paper). This approach leads to the following contributions:

- i. Stability in the operating voltage and current of the bidirectional dc-dc converter, as well as effective ripple reduction in both parameters. This results in a positive impact on the lifetime of ESS systems (e.g. batteries and SCs).

- ii. Easy and practical implementation of the bidirectional dc-dc converter for interconnecting two power sources with high voltage ratios (e.g. ESS systems and RESs).

The implicit benefits of the approach used in the proposed bidirectional dc-dc converter are: personnel safety, reduced electrical noise.

In this article the following sections are presented; in section II a detailed analysis of the converter to be studied is made, as well as the obtaining of the different values of each component of the circuit; in section III the simulation results of such proposed circuit are presented, as well as the power semiconductor devices MOSFETs that were selected; in section IV the respective conclusions of the results obtained are exposed; and in section V the literature used is shown.

### DC-DC Converter Analysis and Design

In order to implement the converter, a steady-state analysis of the converters will be performed separately and in a forward direction (supercapacitor as a load), taking into account that the transistors  $T_3$  and  $T_4$  (see Figure 1) will have duty cycles complementary to  $T_2$  and  $T_1$  respectively, and  $S_3$  y  $S_4$  with respect to  $S_1$  and  $S_2$ ; the simulation results are presented in the following sections.

#### I. Two-Branch Parallel Converter

The two-branch parallel converter as explained above will be used only to decrease the current ripple to near zero percent and as this depends on the direction in which it will be used, then it can operate as a boost or buck converter.

Although in the buck mode and with the phases shifted 180 degrees between the two branches, then the output current ripple can be reduced as far as the duty cycle is increased. The maximum point where the current ripple is almost zero is when the sum of each duty cycle of each branch gives one, i.e., 0.5.

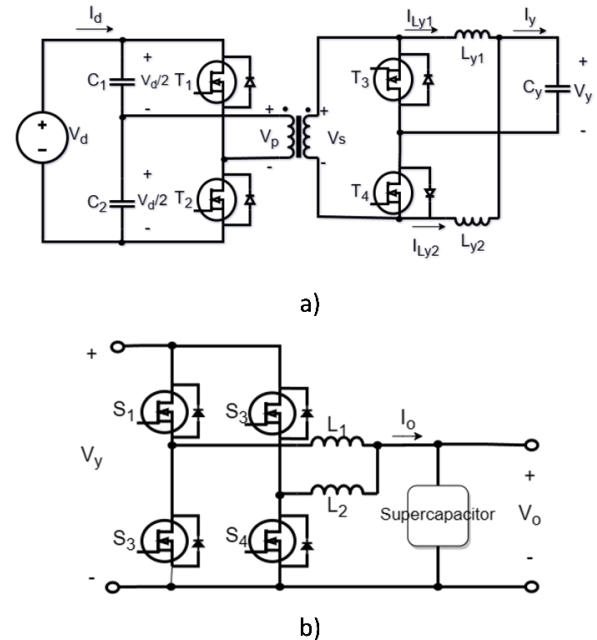


**Figure 1** Schematic diagram of proposed topologies a) half-bridge converter complete with current doubler, b) two-branch parallel converter

Source: Own elaboration

For the design of the proposed converter, its voltage gain will be determined first, taking into account that the phase shift must be 180 degrees and the inductors of the same value, so analyzing one of the branches is more than enough.

When the switch  $S_1$  is on the current flows through it and the transistor  $S_3$  will be off, therefore, the inductor current  $I_{L1}$  is increased. This increase corresponds to a positive slope current ripple at  $L_1$ , which can be determined by the following equation:

$$\Delta i_{L1(ON)} = \frac{1}{L_1} (V_y - V_o) D_2 T_s \quad (1)$$

where  $D_2$  represents the duty cycle,  $T_s$  the switching period,  $V_o$  the output voltage at the supercapacitor and  $V_y$  the input voltage. Now when the switch  $S_1$  is turned off, then the current through the inductor  $L_1$ , is decremented by means of switch,  $S_3$ , resulting in a curl with negative slope, and (2) represents it in mathematical form.

$$\Delta i_{L1(OFF)} = \frac{1}{L_1} (-V_o) (1 - D_2) T_s \quad (2)$$

Since both the increase and decrease in current ripple is of the same magnitude, therefore, the voltage gain can be determined by equating the absolute values of (1) and (2) as defined in (3).

$$\frac{V_o}{V_y} = D_2 \quad (3)$$

## II. Half-Bridge Converter with Current Doubler

The design consists of four transistors ( $T_1$ ,  $T_2$ ,  $T_3$  and  $T_4$ ), two input capacitors ( $C_1$  and  $C_2$ ), one output capacitor ( $C_y$ ) and two output inductors ( $L_{y1}$  and  $L_{y2}$ ) and a transformer with two windings, as depicted in Figure 1B. The duty cycle of the transistors  $T_1$  and  $T_2$  in which it can operate is from 0 to 0.5, above that value a short circuit is caused between them. Since the inductors are connected to the ends of the secondary winding, then their currents will be 180 degrees out of phase, causing the ripple to decrease as the duty cycle increases.

As long as it is held on  $T_2$  a voltage of  $\frac{V_d}{2}$  will be present in the primary, consequently the secondary will have a voltage defined at (4) and the transistor  $T_3$  will remain off, causing in the inductor  $L_{y1}$  an increase of the current  $I_{L_{y1}}$  according to (5).

$$v_s = \frac{N_2 V_d}{N_1 2} \quad (4)$$

$$\Delta i_{L_{y1}(ON)} = \frac{1}{L_{y1}} \left( \frac{N_2 V_d}{N_1 2} - V_y \right) D_1 T_s \quad (5)$$

Taking into account the above considerations, it can be calculated the variation of the current at  $L_{y1}$  as long as  $T_3$  remains in on state (6),

$$\Delta i_{L_{y1}(OFF)} = \frac{1}{L_{y1}} (-V_y)(1-D_1)T_s \quad (6)$$

Performing in a similar way to how it is obtained (3) it is possible to obtain the voltage dc gain from (7).

$$\frac{V_y}{V_d} = \frac{N_2 D_1}{N_1 2} \quad (7)$$

As the two converters (Figures 1a and 1b) are cascaded connected, therefore, the gains are multiplied, thus obtaining the gain between the output and input voltage as,

$$\frac{V_o}{V_d} = \frac{I_d}{I_o} = \frac{1 N_2}{2 N_1} D_1 D_2 \quad (8)$$

Regarding the value of the capacitor, the voltage  $V_y$  ripple must be calculated and for this it must first calculate the ripple of the current  $I_y$ , since in the sum of the current of the inductors the ripple decreases, then according to the Figure 2 the output current ripple is determined from (9).

$$\Delta I_y = \frac{V_y}{L_{y1} f_s} (1-2D_1) \quad (9)$$

Therefore, the ripple of the capacitor is defined as follows (10).

$$\frac{\Delta V_y}{V_y} = \frac{(1-2D_1)}{16L_{y1} C_y f_s^2} \quad (10)$$

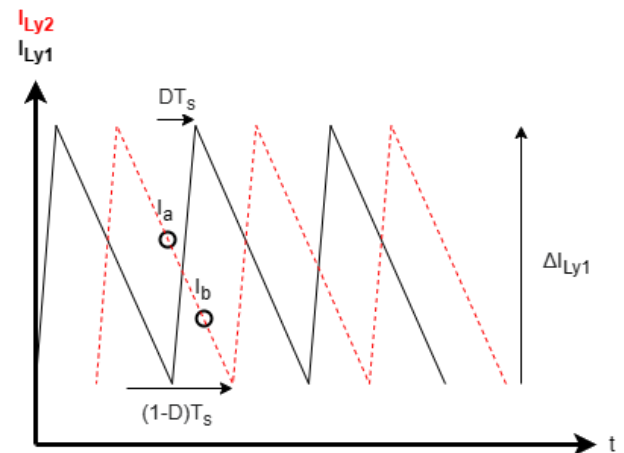


**Figure 2** Variation of the currents with respect to time in inductors  $L_{y1}$  y  $L_{y2}$

Source: Own elaboration

## III. Relationship of Inductor Currents to Output Current

It is easy to deduce from Figure 1 (b) that  $I_o$  is the sum of the currents of the inductors  $L_{y1}$  y  $L_{y2}$  and as both currents have the same waveform, except that they are 180 degrees out of phase; therefore, the average value of the output current is equal to the sum of the two currents of these inductors which leads to significantly reduce the output ripple of  $I_o$  of the two-branch parallel converter.

To obtain a mathematical expression that relates  $I_o$  to the current of  $L_{y1}$ , it is first necessary to know the waveform of current that pass over  $S_3$ , which according to Figure 3 the average current flowing through  $S_3$  can be defined as,

$$I_{S3} = \left[ \frac{1}{2} \Delta I_{L1} (1-D_2) T_s \right] \frac{1}{T_s} + \left[ \widetilde{I}_{L1} (1-D_2) T_s \right] \frac{1}{T_s} \quad (11)$$

Simplifying (11) it is obtained the current in  $I_{S3}$  as shown,

$$I_{S3} = I_{L1} (1-D_2) \quad (12)$$

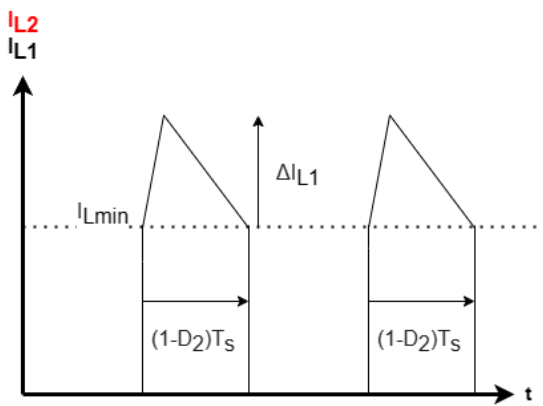


**Figure 3** Current present in transistor  $S_3$ .

Source: Own elaboration

Now for the case of  $I_{L_{y1}}$  it is taken into account that it is half of  $I_y$ ; knowing that the average current in a capacitor is zero, then  $I_y$  is the sum of the currents of  $S_1$  and  $S_2$ , and  $I_{L1}$  is the sum of  $S_1$  and  $S_3$  so this relation is defined by the next equation.

$$I_{L_{y1}} = \frac{D_2 I_o}{2} \quad (13)$$

#### IV. Maximum Transistor Voltages and Currents

This is done in order to determine the worst-case stress on the transistors and thus select the most suitable one. For the analysis it should be assumed that the maximum duty cycle  $D_1$  level is 50%. For the voltages in the transistors  $S_1$ - $S_4$ , it is easy to detect its maximum voltage since it is equal to  $V_y$  for all transistors, on the other hand for the current it is taken into account that when the transistor is in conduction, all the inductor current flows through it and because the inductor current is half of the output current, then this would flow through the transistor, only half of the inductor ripple must be added to obtain the maximum current as,

$$I_{S_{max}} = \frac{1}{2} I_{o_{max}} + \frac{V_o}{4L_1 f_s} \quad (14)$$

The maximum voltage across the switches  $T_1$  and  $T_2$  when they are open is equal to the input voltage of  $V_d$ ; the capacitors also supply current and have the same voltage as the source, so they supply the same amount of current  $I_d$  as the source, so the maximum current is defined as follows,

$$I_{T2_{max}} = I_{T1_{max}} = \frac{1}{4} \frac{N_2}{N_1} I_{o_{max}} \quad (15)$$

From Figure 1 (a) it can be deduced that the maximum stress at  $T_3$  and  $T_4$  is the same as  $V_s$ , that is to say  $\frac{N_2 V_d}{N_1 2}$ . Therefore, the maximum current flowing through these is  $I_y$  as expressed as,

$$I_{T3_{max}} = I_{T4_{max}} = \frac{1}{2} I_{o_{max}} + \frac{N_2 V_d}{8N_1 L_{y1} f_s} \quad (16)$$

#### V. Bidirectional Converter Design

The following design parameters were considered for the calculation of all converter components:

- Input voltage,  $V_d = 100$  V,
- Output voltage,  $V_o = 48$  V,
- Switching frequency,  $f_s = 40$  kHz,
- Output current,  $I_o = 8.5$  A,
- Current and voltage ripples of 5%,
- Transformer turns ratio,  $\frac{N_1}{N_2} = \frac{1}{6}$ .

With the equations defined above (1)-(16) it is determined a duty cycle  $D_1$  of 32%, considering that  $D_2$  is always 0.5. Based on the current relations and the current ripple formulas, the inductances of all the coils can be known, which are for  $L_1$  and  $L_2$  a value of 2.82 mH, and for  $L_{y1}$  and  $L_{y2}$  a value of 15.36 mH, respectively. Finally, the capacitor  $C_y$  which is determined to have a value of 18.31 nF.

For the maximum voltages and currents, a duty cycle of 0.5 and an output current of 10 A are assumed. In the Table 1 it is shown the specifications of the voltage and current values of the power semiconductor devices to which they will be subjected in the bidirectional converter.

Although it must be taken into account that in the reverse operation mode (discharge of the supercapacitor), the proposed converter works as a boost and for a maximum input voltage, the duty cycle must be decreased to zero ( $D_1 = 0$ ), but as physically the converters have a limit point where the voltage starts to decrease. For this reason, a duty cycle of 0.1 was selected to calculate the maximum voltages in the reverse direction of the transistors.  $T_1$ ,  $T_2$ ,  $T_3$  and  $T_4$ , except for the others, since they will work with a fixed duty cycle of 50%.

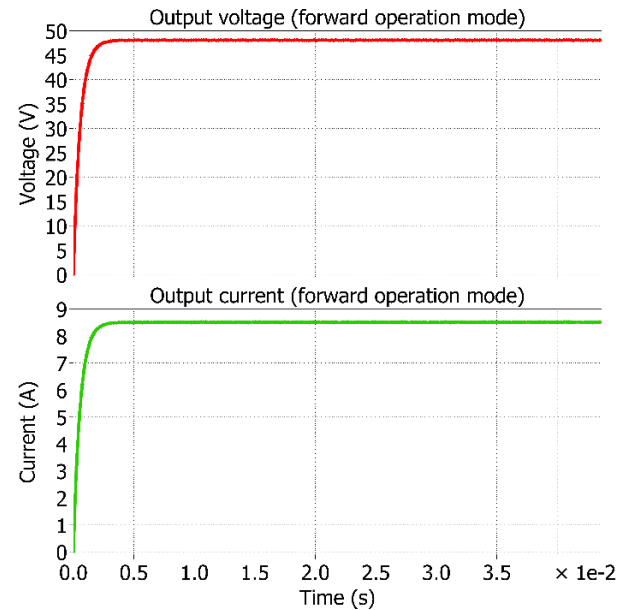
There will be no change in the currents since  $I_o$  is assumed as maximum, so a fuse will be used to avoid over currents.

Transistors	Maximum stresses	Peak currents	Maximum stresses (Reverse)
$T_1$ and $T_2$	100 V	15 A	320 V
$T_3$ and $T_4$	300 V	5.12 A	960 V
$S_1$ and $S_2$	150 V	5.16 A	
$S_3$ and $S_4$	150 V	5.16	

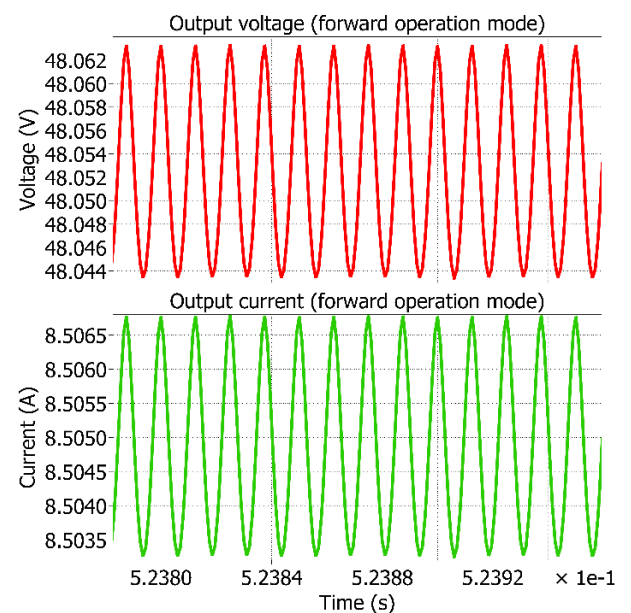
**Table 1** Maximum voltages and currents in the converter  
Source: Own elaboration

## Simulation results

By means of the simulation tool of the PLECS© software, simulation results were performed and obtained, which represent the behavior of the output voltages and currents, as well as of the switches of the proposed converter. These simulations are carried out considering the design parameters and component calculations previously presented. Moreover, it is considered that, during the charging process, the supercapacitor is replaced with a power resistor with a value of  $5.65 \Omega$  in forward direction. Also, the inductor resistances were considered to be  $0.5 \Omega$  for the inductors  $L_y$  and  $0.1 \Omega$  for the inductors  $L$ .



**Graphic 1** Output voltage and current ( $V_o$ ,  $I_o$  respectively)  
Source: Own elaboration



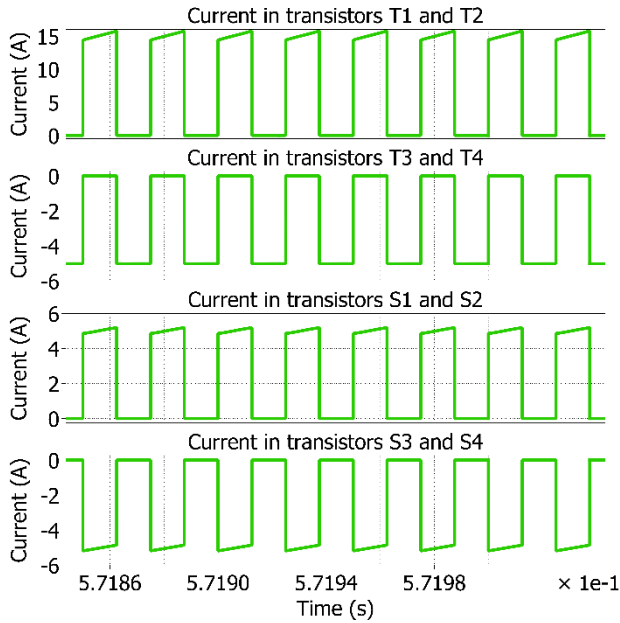
**Graphic 2** Ripples in the output voltage and current (forward direction)  
Source: Own elaboration

Because the converter is configured for minimum ripple, it can be seen Graphic 1 and Graphic 2 (amplified version of Graphic 1), that the desired voltages and currents are being achieved with a ripple of 0.04% for both.

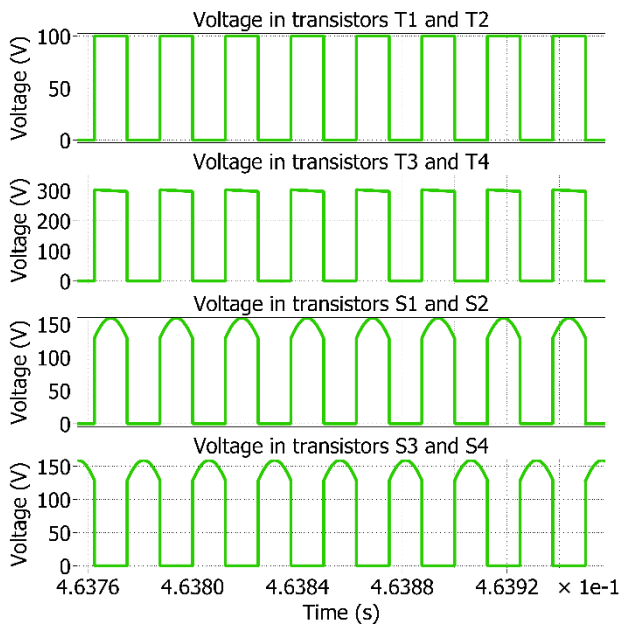
As shown in Graphic 3 and Graphic 4, simulation results confirm that the maximum voltages and currents in the semiconductor devices are similar to those obtained in Table 1.

With this statement, MOSFETs devices can be selected to meet the requirements of the stress voltage and current to which they will be subjected, as well as the switching frequency power semiconductor devices will operate.

In this work, for the switches designated with the letter "T", the semiconductor device CMF10120D was selected, while for the switches designated with the letter "S", the semiconductor device IRF640N was chosen.

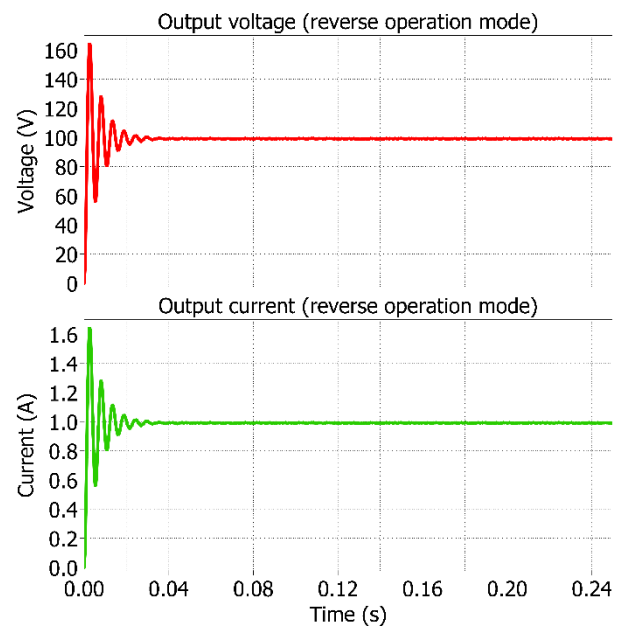


**Graphic 3** Simulation results of currents of transistors T1-T4 and S1-S4, as a variation of time  
Source: Own elaboration



**Graphic 4** Simulation results of voltages of transistors T1-T4 and S1-S4, as a variation of time  
Source: Own elaboration

For the case of the reverse operation of the proposed converter, the same duty cycle was used ( $D_1 = 0.32$ ), but the 100 V input source was eliminated and replaced by a 100  $\Omega$  power resistor, and the 5.65  $\Omega$  was replaced by a 48 V constant voltage source. With the control method by complementary PWMs it is achieved that, for the same duty cycle, the converter is able to operate in two operating directions, as shown in Graphic 5 that prove that can be able to work in discharge mode; Graphic 5 shows the output voltage and current in the resistor of 100  $\Omega$ , that is located in the input of the converter.



**Graphic 5** Simulation results of the output voltage and current of converter operating in the reverse mode. Source: Own elaboration

**Conclusions**

In this work, a bidirectional dc-dc converter for charging and discharging applications of ESS systems (e.g. batteries and SCs) was presented. This converter was designed with an approach based on cascading two dc-dc converters. The first one consisted of an isolated half-bridge dc-dc converter with current doubler and the second one of a two-branch stepped parallel bidirectional. Both converters were driven by complementary PWM modulation, where in the first converter a variable duty cycle was used and in the second a fixed 50% duty cycle. The simulation results and the approach used demonstrated that the proposed converter can stabilize the operating voltage and current during the charging and discharging process management of ESS-based applications (e.g. batteries and SCs).

In addition, an effective voltage and current ripple of 0.04% was achieved. This results in a positive impact on the lifetime of ESS systems. Finally, the approach used leads to an easy and practical implementation of the proposed converter in interconnection applications of two power sources with high voltage ratios (e.g. ESS systems and RESs). The latter, due to the implicit advantages offered by the galvanic isolation of the first converter used in the cascade connection.

### Acknowledgment

Authors would like to thank Tecnológico Nacional de México (TecNM) for the financial support given to this research project under grant number: 13249.21-P.

### References

- Hidalgo-Reyes, J. I., Gómez-Aguilar, J. F., Escobar-Jiménez, R. F., Alvarado-Martínez, V. M., & López-López, M. G. (2019). Classical and fractional-order modeling of equivalent electrical circuits for supercapacitors and batteries, energy management strategies for hybrid systems and methods for the state of charge estimation: A state of the art review. *Microelectronics Journal*, 85, 109–128. <https://doi.org/10.1016/j.mejo.2019.02.006>
- Huang, X., Tang, T., Lv, M., Zhu, Y., & Bao, Q. (2018). Research on the Energy Storage Device of Super Capacitor for Heave Compensation System. *2018 IEEE International Power Electronics and Application Conference and Exposition (PEAC)*, 1–6. <https://doi.org/10.1109/PEAC.2018.8590294>
- Ibanez, F. M., Vadillo, J., Echeverria, J. M., & Fontan, L. (2013). 100kW bidirectional DC/DC converter for a supercapacitor stack. *IEEE PES ISGT Europe 2013*, 1–5. <https://doi.org/10.1109/ISGTEurope.2013.6695246>
- Kayaalp, I., Demirdelen, T., Koroglu, T., Cuma, M. U., Bayindir, K. C., & Tumay, M. (2016). Comparison of Different Phase-Shift Control Methods at Isolated Bidirectional DC-DC Converter. *International Journal of Applied Mathematics, Electronics and Computers*, 4(3), 68. <https://doi.org/10.18100/ijamec.60506>
- Kim, S. M., & Sul, S. K. (2006). Control of rubber tyred gantry crane with energy storage based on supercapacitor bank. *IEEE Transactions on Power Electronics*, 21(5), 1420–1427. <https://doi.org/10.1109/TPEL.2006.880260>
- Lai, C.-M., Yu-Jen Lin, Ming-Hua Hsieh, & Jie-Ting Li. (2016). A newly-designed multiport bidirectional power converter with battery/supercapacitor for hybrid electric/fuel-cell vehicle system. *2016 IEEE Transportation Electrification Conference and Expo, Asia-Pacific (ITEC Asia-Pacific)*, 163–166. <https://doi.org/10.1109/ITEC-AP.2016.7512941>
- Lopez-Flores, D. R., Duran-Gomez, J. L., Herrera-Salcedo, R., & Pineda-Gomez, J. A. (2010). Analysis and design of a simple digital control algorithm for a phase-shift full-bridge DC-DC power converter. *12th IEEE International Power Electronics Congress*, 205–212. <https://doi.org/10.1109/CIEP.2010.5598908>
- Rahimpour, S., & Baghrmian, A. (2017). Bidirectional isolated  $\Gamma$ -source DC-DC converter. *2017 Iranian Conference on Electrical Engineering (ICEE)*, 1378–1383. <https://doi.org/10.1109/IranianCEE.2017.7985257>
- Rico-Secades, M., Lopez-Corominas, E., Calleja, A. J., Quintana, P., Crespo-Iglesias, M., & Garcia-Llera, D. (2016). Improving current equalization in energy storage systems for lighting smart grids applications with the bidirectional one-leg converter. *2016 13th International Conference on Power Electronics (CIEP)*, 339–344. <https://doi.org/10.1109/CIEP.2016.7530781>
- Shreelekha, K., & Arulmozhi, S. (2016). Multiport isolated bidirectional DC-DC converter interfacing battery and supercapacitor for hybrid energy storage application. *2016 International Conference on Electrical, Electronics, and Optimization Techniques (ICEEOT)*, 2763–2768. <https://doi.org/10.1109/ICEEOT.2016.7755198>



Zakis, J., Vinnikov, D., Husev, O., & Rankis, I. (2012). Dynamic behaviour of qZS-based bi-directional DC/DC converter in supercapacitor charging mode. *International Symposium on Power Electronics Power Electronics, Electrical Drives, Automation and Motion*, 764–768. <https://doi.org/10.1109/SPEEDAM.2012.6264554>

Zhixiang Ling, Hui Wang, Kun Yan, & Zaoyi Sun. (2015). A new three-port bidirectional DC/DC converter for hybrid energy storage. *2015 IEEE 2nd International Future Energy Electronics Conference (IFEEC)*, 1–5. <https://doi.org/10.1109/IFEEC.2015.7361598>